4-7-2023

Quantification of Anion and Cation Uptake in Ice Ih Crystals

Tiara Sivells
Baylor University

Pranav Viswanathan
Baylor University

Jenée D. Cyran
Boise State University

The Journal of Chemical Physics ARTICLE scitation.org/journal/jcp

Quantification of anion and cation uptake in ice Ih crystals

Cite as: J. Chem. Phys. 158, 134507 (2023); doi: 10.1063/5.0141057
Submitted: 2 January 2023 • Accepted: 2 March 2023 •
Published Online: 3 April 2023

Tiara Sivells,[1] Pranav Viswanathan,[1] and Jenée D. Cyran[1,2,a)]

AFFILIATIONS

[1] Department of Chemistry and Biochemistry, Baylor University, Waco, Texas 76706, USA
[2] Department of Chemistry and Biochemistry, Boise State University, Boise, Idaho 83725, USA

Note: This paper is part of the 2023 JCP Emerging Investigators Special Collection.
[a)]**Author to whom correspondence should be addressed:** jeneecyran@boisestate.edu

ABSTRACT

While ice has very low solubility for salts compared to water, small amounts of ions are doped into ice crystals. These small ion dopants can alter the fundamental physical and chemical properties of ice, such as its structure and electrical conductivity. Therefore, these results could have a direct impact on the chemical reactivity of ice and ice surfaces. Here, we examine the influence of the uptake of three salts—ammonium chloride (NH_4Cl), sodium chloride (NaCl), and ammonium sulfate [$(NH_4)_2SO_4$]—on ice Ih formation using capillary electrophoresis. Using both cation and anion modes, we observed and quantified the uptake of individual ions into the ice. Our results indicate that anions have a higher propensity for uptake into ice Ih crystals.

INTRODUCTION

Ice is ubiquitous in the environment and plays an essential role in the biogeochemical and atmospheric processes.[1–6] Ice acts as a chemical sink for both organic and inorganic molecules and provides a matrix for exchange of contaminants within the ecosystem.[7–10] Contaminants or chemicals can be accommodated into the solid matrix of ice and induce considerable changes in the properties of the ice.[11–16] For example, Workman and Reynolds discovered in 1948 that an electric charge separation occurred in frozen dilute salt solutions.[17] This charge separation phenomenon is now known as the Workman–Reynolds effect and could play a major role in thunderstorms.[18–20] Furthermore, the interactions between salts and ice are important, as salts can alter the freezing point depression by up to 294 K (Table I).[21]

As aqueous salt solutions freeze, the salts are mostly expelled from the solid phase, saturating the liquid phase with solute and creating brine.[22] Brine rejection has been widely studied for its desalination applications and effects resulting from climate change.[15,23–26] Recent molecular dynamic (MD) simulations, however, have illustrated that not all ions are expelled from the ice crystals.[25,27,28] Interestingly, for NaCl, the Cl^- ions had a higher propensity for inclusion than Na^+. Recent MD simulation results from Berrens *et al.* illustrated a high propensity for Na/Cl ion pairs in the quasi-liquid layer (QLL) on the surface of ice.[12] Despite the previous theoretical simulations, there is a lack of experimental evidence on the inclusion of dopants in ice.

Here, we investigate the uptake of ions from three different salts, sodium chloride (NaCl), ammonium chloride (NH_4Cl), and ammonium sulfate [$(NH_4)_2SO_4$], into ice Ih crystals with capillary electrophoresis (CE). These salts were chosen owing to their environmental relevance. CE provides the ability to detect and quantify both cations and anions and has been utilized to measure trace amounts of ions in water.[29–33] CE also has the benefit of low concentration detection limits, typically on the micromolar scale.[34]

One challenge with many studies involving dopants in ice is the ability to form well-defined crystals in a reproducible manner. To overcome this challenge, single crystalline ice can be produced with dopants.[35] Producing single crystalline-doped ice and understanding fundamental properties, such as dopant concentrations, the localization of dopants in the ice structure, and controlling doping, can provide reproducible samples that can be used to study high impact phenomena, such as proton transfer in ice or the impact of impurities in photochemical reactions in clouds.[36–40]

TABLE I. Uptake concentrations of anions and cations into ice Ih crystals.

Salt		Cation	Anion
NaCl	Core 1	13.13 ± 0.68	15.71 ± 0.81
	Core 2	6.36 ± 0.34	9.87 ± 2.78
	Core 3	7.62 ± 0.37	12.53 ± 1.99
	Core 4	7.34 ± 0.29	10.19 ± 0.99
NH_4Cl	Core 1	3.89 ± 1.20	6.52 ± 1.75
	Core 2	4.62 ± 1.52	8.59 ± 0.22
	Core 3	2.48 ± 0.51	4.17 ± 0.88
	Core 4	1.63 ± 0.02	2.52 ± 0.07
$(NH_4)_2SO_4$	Core 1	19.99 ± 3.87	20.13 ± 3.18
	Core 2	7.96 ± 1.95	6.92 ± 1.76
	Core 3	3.07 ± 0.01	2.01 ± 0.01

MATERIALS AND METHODS

Materials

Ammonium sulfate (99.9999% Suprapur) and ammonium chloride (99.995% Suprapur) were purchased from Sigma-Aldrich, and sodium chloride (≥99.0%) was obtained from VWR. Each salt was dissolved in Millipore water (resistivity: 18.20 MΩ cm) to produce 100 mM solutions for ice growth.

METHODS

Ice growth

A modified Czochralski melt method was used with a custom-built apparatus, as previously described.[11] The apparatus consists of a copper pin attached to a voltage-controlled Peltier to control the temperature. A single-crystalline, basal-oriented ice seed with a diameter of 2.5 cm and a depth of ~3 cm is used to grow the doped ice. The seed is oriented to the basal plane utilizing Formvar etching, where a thin layer of Formvar solution (2% m/v in ethylene dichloride) was applied to a slice of ice and examined under a microscope to verify the orientation, i.e., hexagonal etch pits for the basal plane.[41,42] When the melt bath reached 0.5 ± 0.1 °C, the seed was attached to the copper pin, and a molten layer was created with a heat gun. The seed was then submerged in the melt bath for 60 min before it was extracted out of the melt bath at a rate of 1.3 mm/h. The ice boule was harvested after 23 h. The blank and doped boules were stored at ~253 K for 30 min. The ice boule was examined under two cross polarizers to determine the crystallinity properties.[43] The ice boule was cut into ice cores, as illustrated in Fig. 1. The core of the boule (2 × 1 × 2 cm^3) was melted and placed into a vial. The vials were stored at 277 K and wrapped in parafilm to reduce evaporation.

Capillary electrophoresis

Capillary electrophoresis is an extremely useful analytical technique that can be used for particle separation based on the electrical properties of the analyte. As solution is drawn into a capillary (usually through a pressure-based injection), an electric field is applied to the system to ionize analytes. The electric field also produces an electroosmotic flow (EOF), which controls the overall migration time of charged solutes.[44] Electrodes are employed as part of the apparatus to promote and direct ion migration to the cathode or the anode, based on the induced analyte charge. The migration rate of individual ions depends upon their electrophoretic mobility, which is a function of charge, solution viscosity, and ionic radius. Inorganic ions, which are used in this experiment, are often hard to detect by conventional means. A chromophore-containing buffer that coordinates with these ions can be utilized during the electrophoresis procedure so that ion migration can be monitored with UV–Vis using a stationary probe.

Standards were prepared using a 100 mM stock salt solution. For each salt, 6–8 standards (3 ml) were prepared, ranging from 0.25 to 75 mM. The standards were spiked with a 60 μl internal standard provided in the SCIEX Cation Analysis Kit and SCIEX Anion Analysis Kit. The internal standards used were Li^+ and $C_8H_{15}O_2^-$ for the cation and anion experiments, respectively.

Uptake concentrations for each melted boule were determined using capillary electrophoresis (CE) on a SCIEX P/ACE MDQ Plus system. The SCIEX Cation Analysis Kit and SCIEX Anion Analysis Kit were used for ion separation, along with a 75 μm I.D., 60.2 cm fused-silica capillary fit with an 800 μm aperture.

For cation analysis, the capillary was conditioned by individually rinsing for 1.00 min with lithium conditioner (SCIEX), rinse solution (SCIEX), and cation coating A (SCIEX). Additionally, it was rinsed for 2.00 min with cation coating B (SCIEX) and for 1.50 min with cation separation buffer (SCIEX). All rinses were performed at 20.0 psi. A 5.00 min separation was performed at 30.0 kV (~35.0 μA) with a 1.00 min ramp at normal polarity, followed by a 0.50 min rinse with lithium conditioner and the rinse solution, again at 20.0 psi. For each cation sample, the data collection method consisted of a 0.50 min rinse with cation coating A and cation coating B, respectively, followed by a 1.50 min rinse with the cation separation buffer, all at 20.0 psi. After a 0.20 min pause, the sample was injected for 5.0 s at 0.50 psi, followed by the injection of a water plug (Milli-Q, 18.20 MΩ cm) for 10.0 s at 0.1 psi. Voltage separation is then performed at 30.0 kV for 5.00 min with a 1.00 min voltage ramp at normal polarity, with the current reaching ~35.0 μA. During separation, UV absorbance was collected at 200 nm. After separation, the capillary was again rinsed with lithium conditioner and rinse solution for 0.50 min each at 20.0 psi.

For anion analysis, the capillary was conditioned by rinsing with sodium conditioner (SCIEX) and rinse solution (SCIEX) for 1.00 min each, followed by a 0.50 min rinse with anion coating (SCIEX) and anion separation buffer (SCIEX), respectively. All rinses were performed at 20.0 psi. A 10.00 min separation was performed at 30.0 kV with a 1.00 min voltage ramp with reverse polarity. After separation, the capillary was again rinsed with sodium conditioner and rinse solution for 0.50 min each, at 20.0 psi. For each anion sample, the data collection method consisted of independent rinses with anion coating and anion separation buffer, both at 20.0 psi for 0.50 min. The sample was subsequently injected for 8.0 s at 0.5 psi, followed by the injection of a water plug (Milli-Q, 18.20 MΩ·cm) for 10.0 s at 0.1 psi. Voltage-based separation was then carried out for 8.00 min at 30.0 kV with a 1.00 min ramp at reverse polarity, where the current reached approximately −53.0 μA. UV absorbance

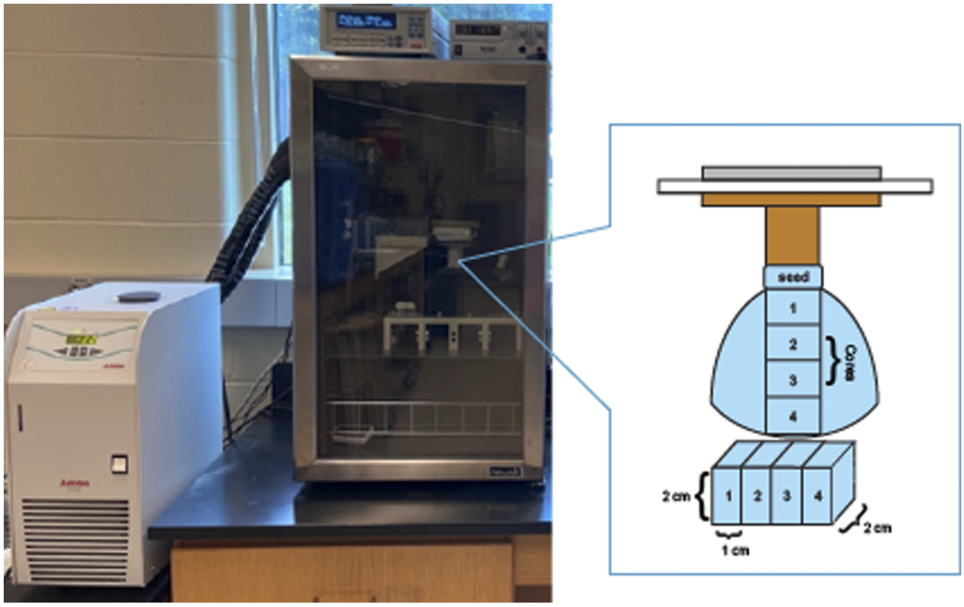

FIG. 1. Image of our custom-made ice growth apparatus and illustration of ice growth and coring of ice boule.

data were collected during separation at 230 nm. Following separation, the capillary was again rinsed with sodium conditioner and rinse solution for 0.50 min each, both at 20.0 psi.

For both cation and anion samples, temperatures were maintained at 298.0 K throughout the data collection. All standards and crystal core samples were collected in triplicate, with two capillary conditioning runs performed between each new sample for thorough cleaning of the capillary.

An electropherogram is collected that displays the migration time of a given peak with a given absorbance. The migration times for the respective ion peaks are cross referenced to the Test Mix provided by SCIEX. Electropherogram data were transferred to MATLAB for processing. The standard and sample data were baseline corrected. A griddedInterpolant function in MATLAB was used to interpolate data points for optimized integration. Peak areas for the desired analyte were integrated, as illustrated in Fig. 2, and the triplicate areas for each standard and sample were averaged. The averaged standard areas were plotted against their concentrations to construct a calibration curve, which was subsequently used as a reference to calculate ion uptake concentrations in each crystal core.

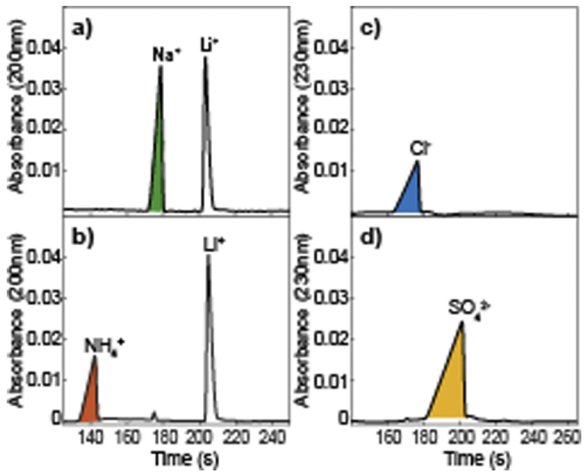

FIG. 2. Representative electropherograms for (a) sodium, (b) ammonium, (c) chloride, and (d) sulfate. An internal standard was used in the cation measurements, thus there is a peak from the ion of interest and the internal standard, Li^+.

RESULTS AND DISCUSSION

The uptake concentrations for the cations and anions in single crystalline ice are illustrated in Fig. 3. We investigated three salts, NaCl, NH_4Cl, and $(NH_4)_2SO_4$, each grown from 100 mM solutions. It should be noted that the concentration of the ammonium ion varies between NH_4Cl and $(NH_4)_2SO_4$ due to the difference in molar ratio, i.e., there is twice as much ammonium in ammonium sulfate

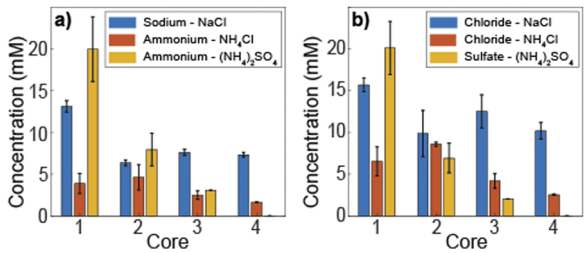

FIG. 3. Uptake concentrations of (a) cations and (b) anions into ice *Ih* crystal cores measured utilizing capillary electrophoresis. Each core is averaged over three samples measured in triplicate, and the error bars indicate the difference between the triplicates.

compared to ammonium chloride [Fig. 3(a)]. Moreover, there are twice as many NH_4^+ ions than SO_4^{2-} in a 100 mM solution. Our experimental results indicate the uptake of anions is higher than that of cations for each of the salts.

Based on the results in Fig. 3, there is higher variability in Core 1 than the other cores. This could be related to the concentration gradient when the seed is initially placed in the bath. The seed is pure H_2O, single crystalline ice oriented to the basal plane. The subsequent cores have less variability, and the uptake concentration decreases. We see an overall increase in the uptake of $(NH_4)_2SO_4$ in Core 1 compared to NaCl and NH_4Cl. This could be due to the increased solubility of $(NH_4)_2SO_4$, which is 71.0 g, while NaCl and NH_4Cl are only 35.7 and 29.7 g, respectively, per 100 g of water at 0 °C.[45] We note that Na^+ was found in the control, blank ice boule, where this concentration was subtracted out of the subsequent ice boule samples for the cation-NaCl. The growth of $(NH_4)_2SO_4$ was slower than that of the other crystals and resulted in only three cores. It should be noted that while the seeds are single crystalline, the doped ice boules are not all necessarily single crystalline and, therefore, the ice grown could be characterized as either a salt hydrate or crystalline ice (Fig. 4). Furthermore, as our study is limited to the quantification and detection of these ions in the doped boules, it cannot be conclusively specified if there are intergranular fillets or micropockets. However, with doped ice samples, a cloudy appearance was observed near the seed, which correlates with the higher uptake of the ions in Core 1.

Our experimental results indicate the uptake of chloride in both sodium chloride and ammonium chloride is higher than the cations. These results align with recent molecular dynamics (MD) simulations that have shown chloride ions are doped into the ice at a higher concentration than sodium ions.[27,46] The incorporation of chloride ions at a higher concentration is due to their size. MD simulations determined that Cl^- replaces two water molecules without completely disrupting the ice lattice, while Na^+ was included within the open cavity of ice.[27] Tsironi *et al.*[46] calculated a radial distribution function that revealed the Cl–O and Na–O distances, and the presence of an additional peak in the Cl–O radial distribution function correlated with the formation of a hydrate that is not seen in the radial distribution function for Na–O. This further explains the increased uptake of Cl^- as the Cl^- becomes encapsulated in the ice. This is in agreement with the propensity of Cl^- to replace water molecules in the structure of ice and sodium ions' occupation of the ice lattice. Sulfate ions have been shown to form contact ion pairs.[47,48] The development of contact ion pairs in the aqueous solutions could contribute to the lower uptake concentration of sulfate as compared to chloride.

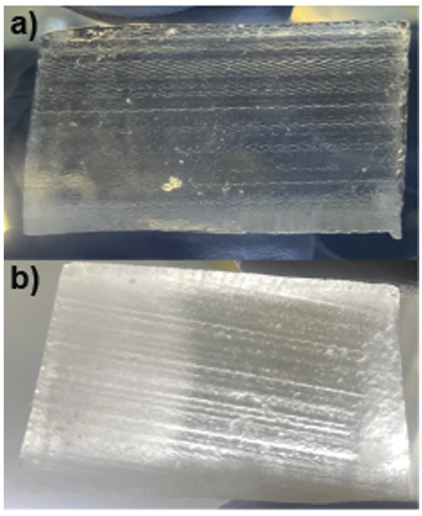

FIG. 4. Illustration of ice cores for (a) a blank ice boule and (b) a doped ice boule.

The partial charges in water contribute to the uptake of the cations, as the size of the ion has little to no effect on the uptake of cations in ice. Instead, Na^+ has a higher uptake than NH_4^+ despite NH_4^+ being smaller in size. This phenomenon could be due to the formation of contact ion pairing. Dong *et al.*[47] determined that the intramolecular bonding within $(NH_4)_2SO_4$ is stronger than the intermolecular bonding between SO_4^{2-} and H_2O. The structure of NH_4^+ has also been known to be included in aqueous solutions that result in hydrogen bonding between NH_4^+ and water molecules.[47,49] In water, many studies have shown that specific molecules behave as "structure makers" and "structure breakers"; however, we have shown that in ice, these molecules have a different effect.[47,50,51] The structure of NH_4Cl has been compared to that of water molecules and has been found to replicate that of water due to the structure of NH_4^+.[47] Interestingly, there is a lower uptake of NH_4^+ in ice when compared to Na^+, which shows a key difference between aqueous solutions and ice. The solubility of these salts in water at 0 °C differs from what is observed with the overall uptake of the salts in ice, where $(NH_4)_2SO_4$ has a higher solubility than all the other salts, followed by NaCl and NH_4Cl, respectively.[52–54]

CONCLUSIONS

In summary, we have investigated the uptake of anions and cations of three salts [NaCl, NH_4Cl, and $(NH_4)_2SO_4$] in ice *Ih* crystals. Our results indicate that there is a higher propensity for anion uptake into ice crystals than cations. This study sets the foundation for future studies utilizing spectroscopic techniques that would provide structural details of the ice crystals with ions accommodated. Furthermore, tuning the growth parameters to control the doping of ice could be fruitful for synthetic chemistry.[55]

ACKNOWLEDGMENTS

We thank Joe McCulloch for excellent technical support. This project was funded by the Welch Foundation (Grant No. AA-2029-20200401).

AUTHOR DECLARATIONS

Conflict of Interest

The authors have no conflicts to disclose.

Author Contributions

T. S. and P. V. contributed equally to this work.

Tiara Sivells: Investigation (equal); Writing – original draft (equal); Writing – review & editing (equal). **Pranav Viswanathan**: Investi-

gation (equal); Writing – original draft (equal); Writing – review & editing (equal). **Jenée D. Cyran**: Investigation (equal); Supervision (equal); Writing – original draft (equal); Writing – review & editing (equal).

DATA AVAILABILITY

The data that support the findings of this study are available from the corresponding author upon reasonable request.

REFERENCES

[1] R. von Glasow, Nature **453**, 1195 (2008).
[2] F. Domine, M. Albert, T. Huthwelker, H.-W. Jacobi, A. A. Kokhanovsky, M. Lehning, G. Picard, and W. R. Simpson, Atmos. Chem. Phys. **8**, 171 (2008).
[3] F. Dominé and P. B. Shepson, Science **297**, 1506 (2002).
[4] J. W. Adams, N. S. Holmes, and J. N. Crowley, Atmos. Chem. Phys. **2**, 79 (2002).
[5] A. Křepelová, T. Huthwelker, H. Bluhm, and M. Ammann, ChemPhysChem **11**, 3859 (2010).
[6] T. F. Kahan, S. N. Wren, and D. J. Donaldson, Acc. Chem. Res. **47**, 1587 (2014).
[7] V. F. Petrenko and R. W. Whitworth, *Physics of Ice* (Oxford University Press, 2002).
[8] D. Nomura, M. A. Granskog, P. Assmy, D. Simizu, and G. Hashida, J. Geophys. Res.: Oceans **118**, 6511, https://doi.org/10.1002/2013jc009048 (2013).
[9] T. Huthwelker, D. Lamb, M. Baker, B. Swanson, and T. Peter, J. Colloid Interface Sci. **238**, 147 (2001).
[10] A. M. Grannas, C. Bogdal, K. J. Hageman, C. Halsall, T. Harner, H. Hung, R. Kallenborn, P. Klán, J. Klánová, R. W. Macdonald, T. Meyer, and F. Wania, Atmos. Chem. Phys. **13**, 3271 (2013).
[11] J. D. Cyran, E. H. G. Backus, M. van Zadel, and M. Bonn, Angew. Chem., Int. Ed. **58**, 3620 (2019).
[12] M. L. Berrens, F. C. Bononi, and D. Donadio, Phys. Chem. Chem. Phys. **24**, 20932 (2022).
[13] S. Chakraborty, A. D. Stubbs, and T. F. Kahan, J. Am. Chem. Soc. **144**, 751 (2022).
[14] K. J. Morenz Korol, I. M. Kumayon, T. F. Kahan, and D. J. Donaldson, J. Phys. Chem. A **125**, 8925 (2021).
[15] H. S. Truong-Lam, S. D. Seo, C. Jeon, and J. D. Lee, Cryst. Growth Des. **21**, 6512 (2021).
[16] S. Alavi and J. A. Ripmeester, J. Chem. Phys. **137**, 054712 (2012).
[17] E. J. Workman and S. E. Reynolds, Phys. Rev. **78**, 254 (1950).
[18] J. M. Caranti and A. J. Illingworth, Nature **284**, 44 (1980).
[19] J. Nelson and M. D. Baker, Atmos. Chem. Phys. **3**, 1237 (2003).
[20] N. Kallay and D. Čakara, J. Colloid Interface Sci. **232**, 81 (2000).
[21] R. E. Dickerson, *Molecular Thermodynamics* (W. A. Benjamin, 1969).
[22] P. K. Rohatgi and C. M. Adams, J. Glaciol. **6**, 663 (1967).
[23] L. Erlbeck, M. Rädle, R. Nessel, F. Illner, W. Müller, K. Rudolph, T. Kunz, and F.-J. Methner, Desalination **407**, 93 (2017).
[24] J. Fournier, J. L. Grange, and S. Vergara, Desalination **15**, 167 (1974).
[25] L. Vrbka and P. Jungwirth, Phys. Rev. Lett. **95**, 148501 (2005).
[26] A. Y. Shcherbina, L. D. Talley, and D. L. Rudnick, Science **302**, 1952 (2003).
[27] M. M. Conde, M. Rovere, and P. Gallo, Phys. Chem. Chem. Phys. **19**, 9566 (2017).
[28] J. S. Kim and A. Yethiraj, J. Chem. Phys. **129**, 124504 (2008).
[29] L. Varden, B. Smith, and F. Bou-Abdallah, J. Chromatogr. Sep. Tech. **8**, 361 (2017).
[30] T. Hiissa, H. Sirén, T. Kotiaho, M. Snellman, and A. Hautojärvi, J. Chromatogr. A **853**, 403 (1999).
[31] H. Sirén and S. Väntsi, J. Chromatogr. A **957**, 17 (2002).
[32] F. Liu, Z. Li, J. Hao, X. Zhou, F. Wang, H. Zhang, P. Wang, X. Zhang, M. Song, and T. Chen, Front. Earth Sci. **8**, 527493 (2020).
[33] F. Borghini and R. Bargagli, Antarct. Sci. **16**, 107 (2004).
[34] C. Johns, M. Macka, and P. R. Haddad, Electrophoresis **24**, 2150 (2003).
[35] P. W. Wilson and A. D. J. Haymet, J. Phys. Chem. B **112**, 11750 (2008).
[36] C. Kobayashi, S. Saito, and I. Ohmine, J. Chem. Phys. **113**, 9090 (2000).
[37] J. H. Chelf and S. T. Martin, J. Geophys. Res.: Atmospheres **106**, 1215, https://doi.org/10.1029/2000jd900477 (2001).
[38] T. F. Whale, J. Chem. Phys. **156**, 144503 (2022).
[39] S. Kataoka, M. Harada, and T. Okada, J. Phys. Chem. C **126**, 8113 (2022).
[40] A. Bergantini, A. L. F. de Barros, N. N. Toribio, H. Rothard, P. Boduch, and E. F. da Silveira, J. Phys. Chem. A **126**, 2007 (2022).
[41] D. v. d. S. Roos, J. Glaciol. **6**, 411 (1966).
[42] M. J. Shultz, A. Brumberg, P. J. Bisson, and R. Shultz, Proc. Natl. Acad. Sci. U. S. A. **112**, E6096 (2015).
[43] P. Bisson, H. Groenzin, I. L. Barnett, and M. J. Shultz, Rev. Sci. Instrum. **87**, 034103 (2016).
[44] H. H. Lauer and G. P. Rozing, *High Performance Capillary Electrophoresis*, 2nd ed. (Agilent Technologies, 2018).
[45] J. W. Mullin, *Crystallization*, 4th ed. (Butterworth-Heinemann, 2001).
[46] I. Tsironi, D. Schlesinger, A. Späh, L. Eriksson, M. Segad, and F. Perakis, Phys. Chem. Chem. Phys. **22**, 7625 (2020).
[47] J.-L. Dong, X.-H. Li, L.-J. Zhao, H.-S. Xiao, F. Wang, X. Guo, and Y.-H. Zhang, J. Phys. Chem. B **111**, 12170 (2007).
[48] Y.-H. Zhang and C. K. Chan, J. Phys. Chem. A **106**, 285 (2002).
[49] H. S. Frank and A. L. Robinson, J. Chem. Phys. **8**, 933 (1940).
[50] C. C. Pye and W. W. Rudolph, J. Phys. Chem. A **105**, 905 (2001).
[51] G. E. Walrafen, J. Chem. Phys. **55**, 768 (1971).
[52] S. Sawamura, N. Yoshimoto, Y. Taniguchi, and Y. Yamaura, High Press. Res. **16**, 253 (1999).
[53] H. Langer and H. Offermann, J. Cryst. Growth **60**, 389 (1982).
[54] Z. Zhu, Z. Zhu, and P. Yin, J. Chem. Eng. Data **53**, 564 (2008).
[55] R. Ruzicka, L. Baráková, and P. Klán, J. Phys. Chem. B **109**, 9346 (2005).